Materials Science and Engineering C 31 (2011) 514–522

Contents lists available at ScienceDirect

Materials Science and Engineering C

journal homepage: www.elsevier.com/locate/msec

The adsorption characteristics of osteopontin on hydroxyapatite and gold

A. Dolatshahi-Pirouz [a], N. Kolman [a], A. Arpanaei [a,d], T. Jensen [a,c], M. Foss [a,*], J. Chevallier [b], P. Kingshott [a], J. Baas [c], K. Søballe [c], F. Besenbacher [a,b]

[a] Interdisciplinary Nanoscience Center (iNANO), Aarhus University, 8000 Aarhus C, Denmark
[b] Department of Physics and Astronomy, Aarhus University, 8000 Aarhus C, Denmark
[c] Orthopaedic Research Laboratory, Aarhus University Hospital, 8000 Aarhus C, Denmark
[d] Department of Industrial and Environmental Biotechnology, National Institute of Genetic Engineering and Biotechnology, P.O. Box: 14965/161, Tehran, Iran

ARTICLE INFO

Article history:
Received 8 April 2010
Received in revised form 17 September 2010
Accepted 18 October 2010
Available online 25 October 2010

Keywords:
Osteopontin
Hydroxyapatite
QCM-D
Protein adsorption
Biomaterials
XPS

ABSTRACT

The adsorption of osteopontin on hydroxyapatite (HA) and reference gold (Au) surfaces was studied at different protein bulk concentrations over the temperature range 295–317 K, using quartz crystal microbalance with dissipation (QCM-D) and X-ray photoelectron spectroscopy (XPS). The QCM-D protein adsorption studies were complemented with polyclonal antibodies to examine the availability of protein sequences on the resulting protein layer. The QCM-D and XPS results show that the osteopontin surface mass uptake is larger on Au as compared to HA surfaces within the range of experimental conditions examined (protein bulk concentrations and temperature range), in accordance with the formation of a more compact protein film on Au. The specific antibody binding to the resulting adsorbed osteopontin layer as measured by QCM-D further confirms that the protein packing and conformational/orientational changes occurring during OPN adsorption on Au and HA are different, since fewer antibodies are observed to bind per OPN molecule on Au as compared to HA. The adsorption process on the respective surfaces was modeled using both the Langmuir and Hill adsorption isotherms, and from these isotherm curves, the Gibbs free energy, ΔG, of the osteopontin adsorption was determined. The estimated ΔG values indicate that the osteopontin molecules have a high affinity towards Au, while a lower affinity is observed between osteopontin and HA. By examining the changes in ΔG as a function of temperature, we additionally find that the osteopontin adsorption on HA and Au is endothermic and driven by an increase in entropy.

1. Introduction

The two main criteria when designing new biomaterials for orthopaedic implants is a fast bone in-growth and a low inflammatory response during the clinical use of the implant [1]. Several different biomaterials such as tantalum, stainless steel and titanium alloys have been introduced [1,2]. However, hydroxyapatite (HA) [$Ca_{10}(PO_4)_6(OH)_2$] is still the most commonly used implant coating in orthopaedic surgery [1], since it leads to a fast bone in-growth and typically generates low inflammation as compared to bare metal implants such as titanium alloys or stainless steel [1,3–6]. The biocompatibility of medical implants is closely related to the initial biological responses mediated by protein and cell attachment on the implant surface [7]. Interfacial attachment of extracellular cell-anchoring proteins such as fibronectin, collagen, osteopontin (OPN), and bonesialoprotein participate in the guidance of osteogenic cells and consequently influence the bone formation on the implant interface [1]. Since HA plays an important role in *in vivo* bone formation and bone remodeling by interacting with proteins such as fibronectin, bonesialoprotein and OPN, it is of great interest to examine the use of these proteins as potential bioactive coatings on HA in order to improve the *in vivo* performance of HA implants even more [1,8–13]. OPN was first recognized in bone in 1985 by Franzen [14] and is known to specifically bind to HA in a favorable orientation and directing the early differentiation of osteoblasts as well as playing an important role in bone mineralization [9,10]. OPN is a highly acidic and phosphorylated protein [10,15] composed of 260–317 amino acids with a molecular weight of 45–75 kDa depending on its origin [14] and has a flexible random coil structure in solution [16]. It contains an arginine–glycine–aspartic (RGD) sequence that is available in solution [16], and specific HA-binding sites (polyaspartic acid motif) [10] which promotes OPN to bind on HA in an extended and activated configuration similar to its native configuration in solution [15]. From a more basic research perspective, the protein adsorption process itself is also of interest, since it is not fully understood how protein concentration, buffer, bulk temperature, surface chemistry and morphology influence protein adsorption, why interfacial protein adsorption remains a very active research area [8,17–28]. Even though the influence of the aforemenioned

* Corresponding author. Tel.: +45 89 42 36 98; fax: +45 89 42 36 90.
E-mail address: foss@inano.au.dk (M. Foss).

0928-4931/$ – see front matter © 2010 Elsevier B.V. All rights reserved.
doi:10.1016/j.msec.2010.10.011

parameters on protein adsorption depends on the system in question, some general features such as surface chemistry facilitated protein conformation and orientational changes are still frequently encountered in the literature [8,17,18,25,26]. For instance it was recently shown in [17] by radiolabelling and cell assay techniques that OPN attaches to NH_2 functionalized surfaces in a different conformation and orientation as compared to COOH functionalized surfaces, and in [8] it was concluded from QCM-D and ellipsometry measurements that an enhanced fibronectin surface activation occurs on HA as compared to Au. Although it is generally accepted that the cell-anchoring domains of OPN are highly active and participate in guiding osteogenic cells when OPN is bound to HA [10,11,16], a comprehensive understanding of the binding mechanism between OPN and HA is still not known in detail. Moreover, several reports tentatively suggest that OPN has a high affinity towards HA [11,12,16,29–32] despite the absence of thorough studies which explore the adsorption characteristics of OPN and HA in detail. Such detailed OPN adsorption studies on 2-D surfaces have been severely hampered by the costly purification process of OPN and the difficulties in obtaining large quantities of the OPN molecule. Here, large quantities of low-cost OPN molecules extracted from bovine milk have been used to examine the adsorption characteristics of OPN on HA and a gold reference surface (Au) by quartz crystal microbalance with dissipation (QCM-D) and X-ray photoelectron spectroscopy (XPS) techniques. The OPN adsorption was investigated at several concentrations and different temperatures in the range 295–317 K with the purpose of determining the changes in Gibbs free energy from the recorded OPN adsorption isotherm curves.

2. Materials and methods

2.1. Proteins and antibodies

Osteopontin (OPN) was purified [33] from bovine milk by Arla Foods Amba, Denmark. The standard grade bulk OPN is highly phosphorylated and consists by weight of 30% full length (35 kDa) and 70% cleaved immediately downstream of the cryptic integrin binding sequence (25 kDa). Moreover polyclonal rabbit OPN antibodies were kindly provided by Esben Skipper Sørensen, Department of Molecular Biology, Aarhus University, while goat anti-albumin antibodies for unspecific binding were purchased from Sigma-Aldrich (Denmark). The OPN proteins were dissolved in a 10 mM Tris buffer with 1 mM $CaCl_2$ and 100 mM NaCl adjusted with HCl and NaOH to pH = 7.82 at 22 °C to the concentrations, $5.5\cdot10^{-7}$ M (15 μg/ml), $1.1\cdot10^{-6}$ M (30 μg/ml), $2.2\cdot10^{-6}$ M (60 μg/ml), $3.2\cdot10^{-6}$ M (90 μg/ml), $3.6\cdot10^{-6}$ M (100 μg/ml), $1.8\cdot10^{-5}$ M (500 μg/ml), $3.6\cdot10^{-5}$ M (1000 μg/ml) and $3.6\cdot10^{-4}$ M (10,000 μg/ml) and the antibodies at $1.1\cdot10^{-5}$ M (300 μg/ml). OPN solutions were kept in a refrigerator for no more than seven days prior to use, while the dissolved antibodies were kept at 4 °C for a maximum of three months. During that period of time no sign of protein/antibody degradation was observed in the QCM-D measurements.

2.2. Quartz crystal microbalance with dissipation (QCM-D)

Quartz crystal microbalance with dissipation (QCM-D) is a versatile technique for monitoring the dynamics of protein adsorption as well as the viscoelastic properties (dissipation) of the resulting protein films on surfaces [8,27]. The QCM-D technique relies on changes in the resonance frequency of a quartz crystal mechanically oscillating in a shear mode, where the change in resonance frequency is related to changes in the adsorbed mass on the crystal [34]. In the case of adsorption of a thin non-dissipative layer with no slip, the frequency shift and the adsorbed surface mass density, Γ_{QCM-D}, are proportional as revealed by the simple Sauerbrey equation [34]:

$$\Gamma_{QCM-D} = -\frac{C}{n}\Delta f_n, \tag{1}$$

where C is the mass sensitivity constant (17.7 ng/cm^2/Hz for a 5 MHz crystal), n (1, 3, 5…) is the overtone number, and Δf_n is the frequency shift of the n'th overtone. In addition to the frequency shifts, the corresponding shift in dissipation, ΔD, is also obtainable by QCM-D, with the dissipation defined as

$$D = \frac{E_{lost}}{2\pi\cdot E_{stored}}. \tag{2}$$

where E_{lost} is the energy dissipated during each oscillation cycle, and E_{stored} is the total energy of the system. The simple Sauerbrey equation is typically considered applicable when the 1/n scaling in (1) is fulfilled and the QCM-D monitored dissipation shift is low. In the following, the 7th overtone (n = 7) was chosen whenever the Sauerbrey equation was employed in the subsequent data analysis, since the 7 overtone provides both an appropriate measurement sensitivity perpendicular to the surface plan (z-direction) as well as very stable and reproducible measurements as compared to lower overtones. In the case of a very dissipative system the simple Sauerbrey Eq. (1) is no longer valid, and it is necessary to use more elaborate complex models, such as the Voight model [35]. Since the QCM-D technique is based on measuring mechanical oscillations, the frequency shift is not only associated with the resulting mass uptake of the proteins on the surface, but it also measures the coupled water (hydration) of the proteins and trapped water in the pores of the protein film [36–39]. All the QCM-D experiments were carried out at a flow rate of 500 μl/min lasting 1 min, resulting in a dispense volume at 500 μl at the temperatures 295 K, 310 K and 317 K using a Q-Sense AB E4 system. In order to assure that the surfaces were completely saturated, an extra OPN injection was made on both Au and HA after the frequency curve had leveled off. None of these extra OPN injections led to significant frequency changes.

2.3. X-ray photoelectron spectroscopy (XPS)

We used XPS to characterize the dry mass on the QCM-D crystal surfaces after OPN adsorption, using a Kratos Axis Ultra^{DLD} instrument equipped with a monochromated $Al_{k\alpha}$ X-ray source ($h\nu = 1486.6$ electron volts (eV)) operating at 15 kV and 10 mA (150 W). A hybrid lens mode was employed during analysis (electrostatic and magnetic), with an analysis area of approximately 300 μm × 700 μm. Wide energy survey scans (WESS) were obtained over the range 0–1400 eV (Corresponding to binding energy) at a pass energy of 160 eV, and used to determine the surface elemental composition. The intensity of the individual XPS peaks corresponding to the individual elements present on the surfaces with XPS was converted into atomic concentrations with the sensitivity factors proposed by the Vision 2 software package supplied with the Kratos Axis Ultra^{DLD} spectrometer. After each QCM-D experiment the quartz sensor crystals were removed from the QCM-D chamber, rinsed with MilliQ water for 60–90 s to remove buffer salts, gently dried with nitrogen gas and subsequently analyzed with XPS. Initial XPS compositional analysis of the Au and HA sensor surfaces showed no presence of nitrogen, and accordingly we thus assume that the nitrogen content measured from the respective protein coatings are solely related to the OPN protein. Even though XPS is a very reliable technique, it is important to recognize that the protein film is removed from its natural solvent environment, dried and put into a high vacuum, circumstances which are known to alter the protein film significantly. Therefore, the QCM-D technique was chosen for the detailed examination of OPN interaction with Au and HA, and XPS was only used to estimate the water content in the respective protein films.

2.4. Characterization of the surfaces

Quartz crystal microbalance crystals (AT-cut) coated with 100 nm Au (QSX 301) or a 10 nm layer of HA electrodeposited on top of a titanium adhesion layer (QSX 327) were purchased from Q-Sense AB, Sweden. The root-mean-square roughness (RMS-value) as defined in [40] was determined by atomic force microscopy (AFM). The AFM images were acquired in tapping mode at scan frequencies 1–2 Hz under ambient conditions applying a silicon cantilever (NSG01, NT-MDT, Moscow, Russia) with a typical resonance frequency around 150 kHz, a spring constant of 5.5 N/m and a tip radius below 10 nm. The AFM images (512×512 pixels) were all quadratic with linear dimensions of 1 μm, 3 μm and 5.5 μm. The RMS roughness remained constant as function of image size indicating that the RMS roughness was saturated in this length scale regime [40]. All surfaces used in the protein and contact angle measurements were ozone-cleaned with UV (Bioforce, Ames, CA, USA) for 25–30 min. prior to each experiment.

2.5. Statistical analysis

At least three measurements were carried out for each type of experiment, and the average value for each experiment was subsequently calculated and presented as mean ± standard error-of-mean value.

3. Result and discussion

3.1. Surface characterization

By analyzing the AFM images with SPIP (Image Metrology A/S, 2800 Ks. Lyngby, Denmark, see www.imagemet.com), RMS-values of 1.03 ± 0.11 nm on Au and 2.3 ± 0.2 nm on HA were obtained, while the surface increase as compared to an atomically flat surface was 0.45 ± 0.08% on Au and 1.3 ± 0.3% on HA. As seen from the AFM images in Fig. 1, both surfaces consisted of grainy features. However, the HA surface also consisted of deep pores, which most likely contribute a great deal to the RMS-value and surface area increase observed on HA. Since these pores only cover a small part of the surface, it is unlikely that they influence the adsorption outcome significantly. Studies have shown that the adsorption of proteins is not dramatically influenced when the surface roughness is increased by several factors [41,42]. Moreover, a recent study has shown that there is a lower limit which determines when the surface roughness influences the adsorption outcome in a significant manner [42]. Even though a two-fold increase in the RMS-values was observed on HA as compared to Au, the RMS-values are very low, and consequently it is plausible to assume that the different RMS-values found on Au and HA are less important in the adsorption process.

The HA coatings were also investigated by the grazing incidence X-ray diffraction (XRD) technique, and several peaks which belong to the crystalline phase of HA were observed alongside with the peaks from the supporting titanium layer below the HA coating (Fig. 2). From these peaks we can conclude that the HA coating has a crystalline phase. Moreover, we also carried out a dissolution test on the HA coatings by injecting Tris buffer in the QCM-D chambers and examining the QCM-D response over a time span of 30 h, and no sign of thin film degradation was observed from the recorded QCM-D frequency. The wetting behavior of the surfaces was determined by measuring the contact angle using the contact angle instrument model DSA100 (Krüss, Borssteler Chaussee, Hamburg), and both the HA and Au coatings were found to be highly hydrophilic after UV treatment with a contact angle below 10°.

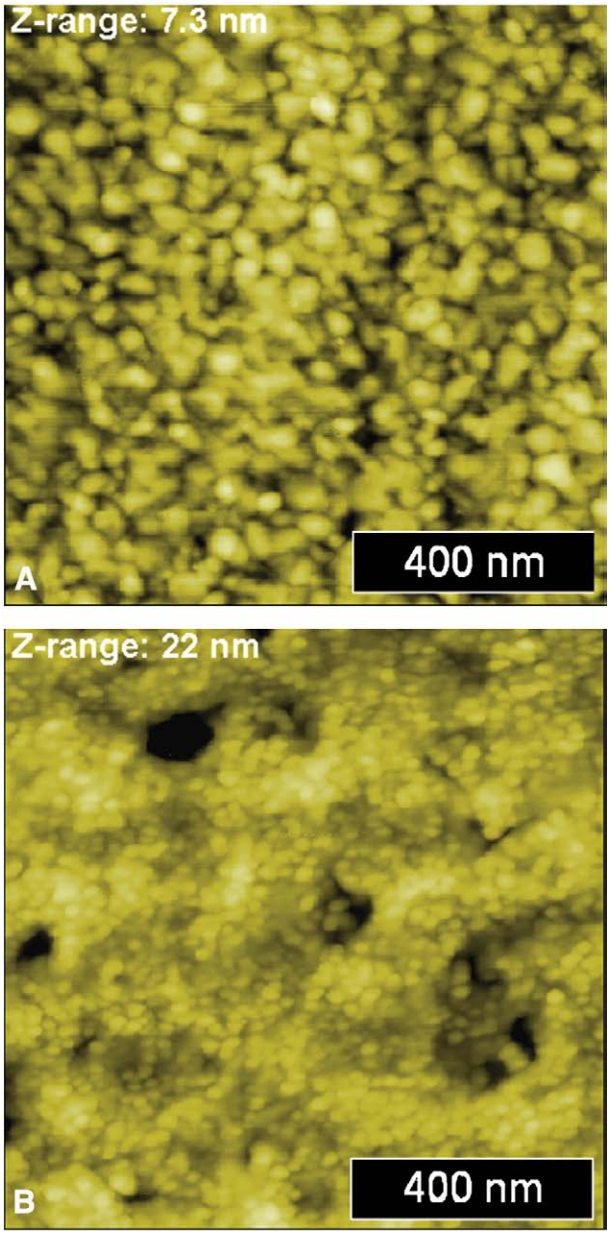

Fig. 1. Representative AFM images of the Au (A) and HA (B) surfaces.

3.2. Osteopontin adsorption monitored by QCM-D

In Fig. 3, representative QCM-D data for OPN adsorption on Au and HA at the bulk concentration 100 μg/ml are shown at the overtone n = 7 after a baseline has been established.

Moreover, the injection of antibodies after the OPN adsorption is shown as well. On both the Au and HA surfaces an instantaneous decrease in frequency and increase in dissipation are observed after the OPN injection in accordance with the addition of additional mass on the quartz crystal sensor surface. The measured QCM-D frequency shifts were subsequently converted to surface mass density values (ng/cm^2) using the simple Sauerbrey Eq. (1) and plotted against the protein bulk concentration to generate adsorption isotherms (see Fig. 4). Frequency to mass conversions using the Sauerbrey equation (Eq. (1)) has been employed in several studies, and the Sauerbrey equation is considered valid when the overtones overlap after scaling with the corresponding overtone numbers, and the dissipation values are low [8,27,36]. In the present study, the dissipation shifts and the

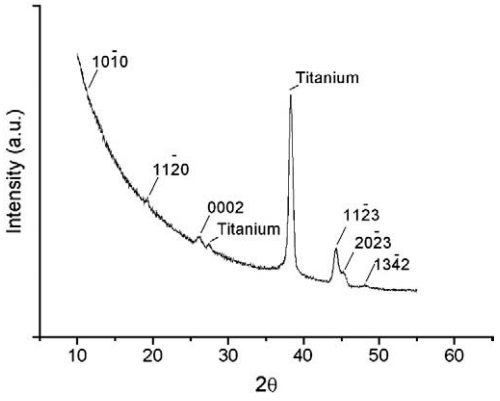

Fig. 2. The regular noise level decreasing from left to right is reflection of X-rays owing to the low angle of incidence. The intensity peaks made distinct with the software applied with the apparatus are marked with the matching diffraction plane from HA. Peaks from the underlying titanium are present. Usually three specific peaks/planes are considered sufficient to identify a crystal. In this measurement 6 peaks specific to HA are identified using unit cell parameters a = 9.43 Å and c = 6.88 Å [43] and it is thus concluded that the surface coating contains crystalline HA.

maximum variation between the scaled overtones in the QCM-D experiments were quite small. Moreover the difference between the Sauerbrey and the Voight estimated surface mass densities was below 15%. Accordingly the simple Sauerbrey equation provides an appropriate first order approximation of the amount of OPN adsorbed to the different surfaces. From Fig. 4 it is observed that the OPN surface mass density increases as a function of protein bulk concentration on both Au and HA. However, the surface mass density values were always larger on Au regardless of the examined experimental conditions (temperature and concentration). From a low protein bulk concentration ($<3.6\cdot10^{-6}$ M = 100 μg/ml) a gradual increase in the QCM-D measured OPN surface mass density ($\Gamma_{QCM\text{-}D}$) is seen as a function of concentration. At higher concentrations the observed increase in surface mass density values slowly levels off. On Au a plateau is reached, while the OPN surface mass uptake never completely reaches a plateau on HA in the measured concentration range. This is particularly noticeable in the experiments carried out on the HA surfaces at T = 295 K. In order to observe the same declination in the OPN surface mass density as observed on Au and HA at bulk temperatures T > 295 K, protein adsorption experiments at extremely high concentrations ($3.6\cdot10^{-4}$ M = 10,000 μg/ml and $3.6\cdot10^{-3}$ M = 100,000 μg/ml) were necessary on HA at T = 295 K (see insets in Fig. 4). Since additional OPN injections were not followed by more OPN adsorption (see materials and method section), this behavior is most likely not caused by multilayer formation or aggregation of the OPN molecules on HA, but rather rearrangement effects (conformational and orientational) leading to a larger protein foot-print at lower protein bulk concentrations as the incoming protein flux on the surface decreases. The changes in surface mass density with varying protein bulk concentrations indicate that protein–protein interactions and/or post adsorption protein rearrangements, i.e. conformational and geometrical, play an important role during the adsorption process. Assuming that the same amount of water is bound to the protein films formed on Au and HA, the results presented in Fig. 4 suggest that a higher OPN surface mass density is achieved on Au as compared to HA. To confirm these interesting findings, additional experiments were designed to investigate if the same amount of water actually bound to the respective OPN protein films on Au and HA under the different experimental conditions.

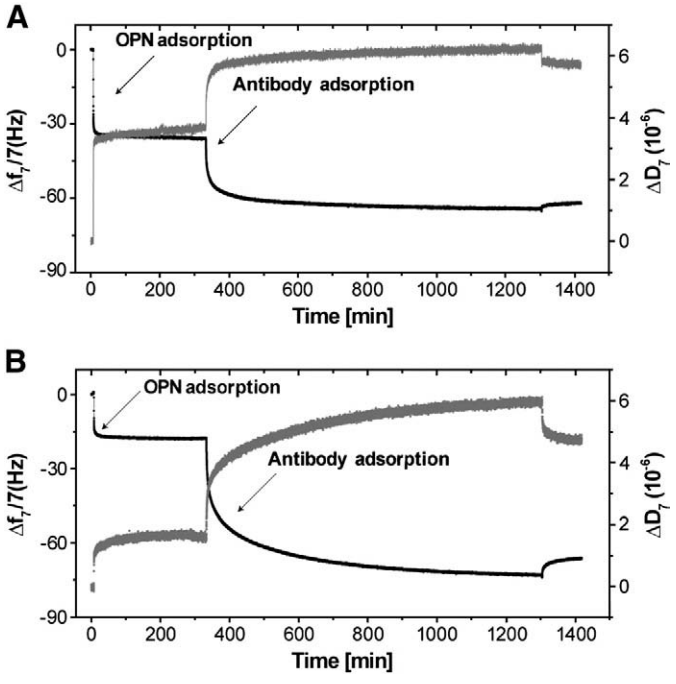

Fig. 3. Representative QCM-D curves showing the change in dissipation, ΔD (grey), and frequency shift, Δf (black), during adsorption of 100 μg/ml osteopontin (OPN) after a baseline have been established, followed by a buffer rinse (Tris) and a consecutive OPN antibody injection on (A) Au and (B) HA.

3.3. Determination of protein dry mass using X-ray photoelectron spectroscopy (XPS)

The influence of bound water on protein adsorption results obtained by QCM-D (Fig. 4) was investigated by the XPS technique on selected Au and HA surfaces with preadsorbed OPN at varying concentrations and temperatures. The XPS technique probes the outer 2–10 nm of the surface depending on the emission angle of the sample, and in the past the technique has been used extensively to examine protein adsorption on surfaces [44,45]. Assuming that a uniform protein layer has formed on the surface, it is possible to determine the effective thickness of the protein layer by measuring the intensity of the nitrogen 1 s peak (I_N) from the following equation [45].

$$\frac{I_N}{I_\infty} = 1 - e^{-\frac{d}{\lambda \cos\phi}} \quad (3)$$

Here I_N is the atomic percentage of nitrogen present on the surface, and I_∞ the nitrogen content (%) in an infinitive thick protein layer, ϕ the photoelectron emission angle measured relative to the surface normal, d the thickness of the adsorbed protein layer and λ the inelastic mean free path (IMFP) of the N1s photoelectrons. The photoelectron emission angle was fixed at 0° allowing a maximum probe depth (10 nm), and the λ value was estimated to be 2.36 nm using a free software package available online [46] with 1088 eV as the energy of the N1s photoelectrons. The nitrogen content (%) of an OPN molecule was determined to be 14.45 ± 0.16 from the analysis of a thick film of OPN deposited on gold, which is sufficient to completely attenuate the underlying gold signal. This was carried out by solution casting a concentrated aliquot (1000 μg/ml) of OPN diluted in MilliQ water onto a gold surface and allowing it to dry overnight followed by XPS analysis. The protein layer thickness values acquired from Eq. (3) was subsequently transformed to surface mass density values, Γ_{xps} (see Table 1), using the generally accepted density value for proteins 1.35 g/cm^3 [47] as the average density of the protein layers formed on Au and HA. As seen from Table 1, the XPS results show the same trend as observed from the QCM-D measurements, with a larger surface mass uptake on the Au surface. However, the difference in the surface mass uptake is even

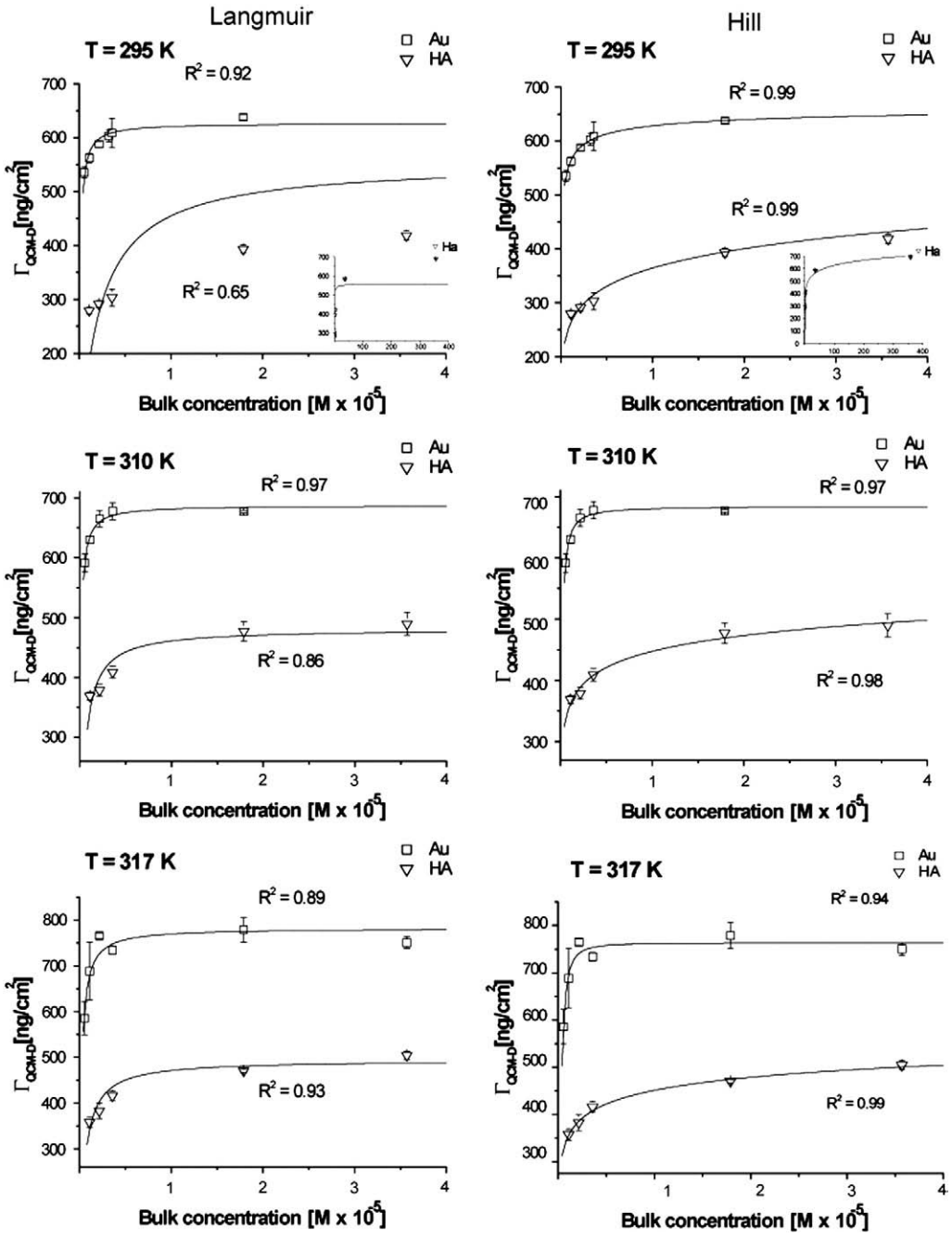

Fig. 4. The QCM-D results are plotted together with the protein bulk concentration to investigate the OPN adsorption isotherms. For the protein experiments with high protein bulk concentrations at the temperature 295 K small insets are attached to the figures showing the adsorption isotherm behavior at these extremely high concentrations. The surface mass density $\Gamma_{QCM\text{-}D}$ (ng/cm^2) increases with higher bulk concentrations, gradually leveling off as the concentration is increases. The results are fitted with both the Langmuir (left) and the Hill equation (right), and the goodness of each fit (r^2) is indicated as well.

more apparent from the XPS results, which seems to indicate that more water was coupled to the OPN protein films formed on HA. The relative amount of water coupled to the respective protein films (water factor) was determined as the ratio between the observed QCM-D and XPS surface mass densities ($\Gamma_{QCM\text{-}D}/\Gamma_{xps}$), and depicted in Table 1. As anticipated a larger water factor is found on HA as compared to Au regardless of the experimental conditions. Interestingly, the water factor was comparable on Au at different protein bulk concentration and temperatures attaining values from 1.43 to 1.96, when taking the uncertainties into account. This suggests that the amount of water coupled to the protein films on Au was not strongly influenced by these particular conditions, in accordance with recent publications on the adsorption of fibronectin on Au and HA [8]. The same trend is also seen for the water factors found on HA under different conditions, however, a slightly lower and similar water factor within the uncertainties is observed at T = 295 and 317 K ranging from 2.73 to 2.90 as compared to T = 310 K, where the water factor attained the values 3.01–3.60. We can thus conclude that the amount of water in the respective OPN films depends strongly on the surface chemistry (Au or HA), while it is less dependent on the protein bulk concentration. The water binding capability of protein films is influenced by both the conformation of single proteins on the surface and the arrangements of the individual protein molecules in the protein layer [36–39]. The difference in the

Table 1
A summary of the XPS (Γ_{XPS}) and QCM-D ($\Gamma_{QCM\text{-}D}$) surface mass densities on Au and HA at different bulk temperatures and concentrations together with the water factor ($\Gamma_{QCM\text{-}D}/\Gamma_{XPS}$).

Surface	Temperature [Kelvin]	Protein concentration [μM]	$\Gamma_{QCM\text{-}D}$ [ng/cm^2]	XPS thickness [nm]	Γ_{XPS} [ng/cm^2]	Water factor ($\Gamma_{QCM\text{-}D}/\Gamma_{xps}$)
Au	295	3.6	608 ± 11	2.64 ± 0.16	356 ± 22	1.71 ± 0.11
Au	295	18	638 ± 5	3.30 ± 0.52	445 ± 71	1.43 ± 0.23
Au	310	0.6	630 ± 6	2.50 ± 0.19	337 ± 26	1.87 ± 0.15
Au	310	1.1	665 ± 14	2.77 ± 0.23	374 ± 31	1.78 ± 0.15
Au	310	18	678 ± 2	3.23 ± 0.79	436 ± 107	1.56 ± 0.38
Au	317	18	779 ± 27	3.0 ± 0.3	405 ± 37	1.93 ± 0.19
Au	317	36	752 ± 14	2.84 ± 0.15	384 ± 20	1.96 ± 0.11
Ha	295	3.6	303 ± 16	0.80 ± 0.02	107 ± 3	2.83 ± 0.17
Ha	295	18	393 ± 7	1.04 ± 0.04	141 ± 5	2.79 ± 0.11
Ha	295	36	417 ± 16	1.13 ± 0.06	153 ± 8	2.73 ± 0.18
Ha	310	1.1	379 ± 10	0.93 ± 0.05	126 ± 6	3.01 ± 0.16
Ha	310	18	477 ± 16	1.0 ± 0.04	135 ± 5	3.53 ± 0.18
Ha	310	36	496 ± 22	1.02 ± 0.06	138 ± 8	3.60 ± 0.26
Ha	317	18	474 ± 5	1.24 ± 0.012	167 ± 2	2.84 ± 0.05
Ha	317	36	505 ± 9	1.29 ± 0.02	174 ± 6	2.90 ± 0.11

measured water amount on Au and HA thus suggests that the detailed structure of the protein layers is different on Au as compared to HA. This finding is in accordance with the larger dry OPN surface mass uptake (Γ_{xps}) observed on Au as compared to HA (see Table 1).

3.3. OPN adsorption isotherms

For a fixed surface chemistry (Au or HA) and bulk temperature, the water factor of the respective adsorbed protein layers was almost constant at the protein bulk concentrations examined. The QCM-D results presented in Fig. 4 can therefore be employed directly to discuss adsorption isotherms on Au and HA. Typically the Langmuir adsorption isotherm theory is used for this purpose. The Langmuir model is applicable provided that (a) only one type of adsorption binding is available on the interface, (b) the adsorption process is fully reversible, and (c) interactions between the adsorbents are negligible [45]. The Langmuir equation, which describes the protein surface mass uptake, Γ, as function of the protein bulk concentration, c [8,20–25,48–52], is given by:

$$\Gamma = \frac{\Gamma_{max} K_L c}{1 + K_L c} \tag{4}$$

Here K_L is the Langmuir equilibrium binding constant, a measuring unit for the affinity of the adsorbent towards the sorbent, and Γ_{max} is the surface mass density of the protein at its full monolayer coverage. In most cases protein adsorption is irreversible and protein–protein interactions such as the electrostatic, hydrophobic and van der Waal forces are non-negligible [45]. The Hill equation, however, takes both the presence of different adsorption sites and interactions among the proteins on a given surface into account, and accordingly copes with some of the shortcomings in the more simple Langmuir adsorption theory [45,52]:

$$\Gamma = \frac{\Gamma_{max} K_h c^n}{1 + K_h c^n} \tag{5}$$

where K_h and n are the Hill equilibrium binding constant and the Hill coefficient, respectively. A Hill plot also represents a more complex interaction scheme known as cooperative adsorption [53], where the Hill coefficient, n, describes the degree of cooperativity present during the adsorption. Protein adsorption is cooperative when $n>1.0$, indicating that protein–protein interactions are attractive. On the other hand $n<1.0$ implies that the protein adsorption is non-cooperative and net repulsive forces exist between the adsorbed proteins [51,53]. In the special case, $n=1.0$, the Hill equation is identical to the Langmuir equation [42,51]. From a detailed analysis of adsorption isotherms within the Langmuir and Hill schemes the thermodynamics behind the protein adsorption process can be addressed, since the equilibrium binding constant is related to Gibbs free energy ΔG^0 through

$$\Delta G^0 = -RT\, ln(K) = \Delta H^0 - T\Delta S^0, \tag{6}$$

where R is the ideal gas constant, T the temperature, ΔH^0 the enthalpy change, ΔS^0 the entropy change and K a dimensionless quantity set to K = equilibrium binding constant (Hill (K_h) or Langmuir (K_L)) × $C_{solvent}$ where $C_{solvent}$ is the molar concentration of the solvent, which is 55.5 M (molar concentration of water) [22,24]. The enthalpy change ΔH in a protein adsorption system arises from changes in protein–solvent, protein–protein and protein–surface interactions. The entropy change is however slightly more complex and depends on the degree of freedom in the orientation/conformation of proteins on the surface as well as changes in the protein hydration shell after surface adsorption has occurred [20,54,55]. As seen from Eq. (6), it is also possible to gain an understanding of the changes in enthalpy and entropy change by monitoring the changes in Gibbs free energy as function of temperature T. This is typically done within the context of a rewritten version of Eq. (6) [8,20–25]:

$$ln(K) = -\frac{\Delta H^0}{RT} + \frac{\Delta S^0}{R} \tag{7}$$

Inspired by previous studies [20–25,51,53,56–58], the QCM-D wet mass results presented in Fig. 4 were analyzed within the framework of Eqs. (4) and (5). From the Langmuir fits in Fig. 4 and the corresponding correlation coefficients, R^2, it is clearly revealed that adsorption isotherms on Au and HA do not follow the simple Langmuir model. The Hill equation, on the other hand, provided a very good fit to the protein adsorption data on both Au and HA with R^2 values close to 1, and the Hill coefficients corresponding to the different fits are presented in Fig. 4. Higher Hill coefficient values on Au as compared to HA are observed in Fig. 5, which indicates that protein–protein interactions are more attractive on Au than on HA. Moreover, a clear correlation is revealed between the Hill coefficient n and the adsorption temperature T on Au with an increase in the n value from n = 0.44–1.70 in the temperature range (295 K–317 K), while n stays approximately constant at 0.20–0.25 for the OPN adsorption on the HA surfaces within the same temperature range. In general lower n values are observed on HA as compared to Au, which suggests that the repulsive forces are more important between the OPN molecules adsorbed on HA as compared to the situation on Au, in accordance with a different surface OPN conformation/orientation on Au, since this could lead to an exposure of otherwise hidden sites.

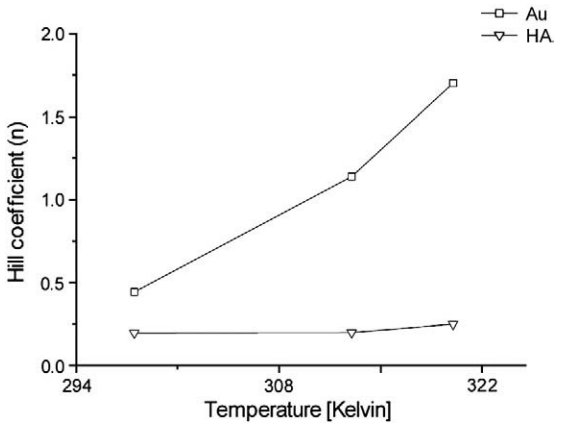

Fig. 5. The hill coefficient (n) on gold (Au) and hydroxyapatite (HA) as a function of temperature.

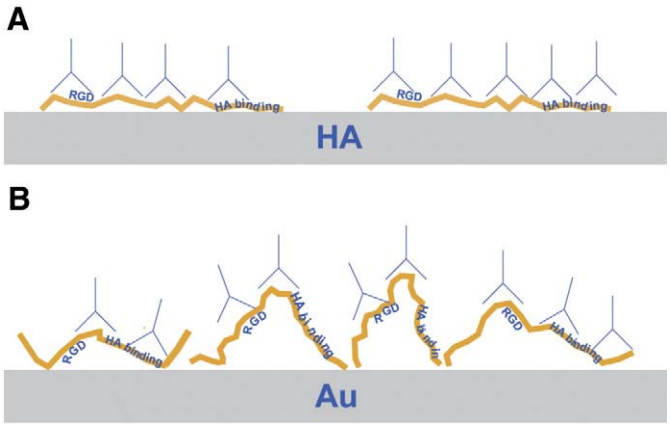

Fig. 7. Illustration of A) how the specific binding facilitated between the HA-binding site on OPN and HA constrains the OPN molecules to bind onto the HA surface in an unfolded configuration leading to a lower entropy state, while B) the OPN random coil is allowed to explore different configurations on Au both conformation and orientation wise leading to a more flexible OPN protein film in accordance with a higher entropy state.

This finding also supports the conclusion made in the previous sections that no OPN multilayers are formed. Since the Langmuir model did not fit the adsorption isotherms in Fig. 4 very well, we chose to rely on the equilibrium binding constant values determined from the Hill fits. These are subsequently plotted against the temperature T. The positive $\ln(K_h)$ values in Fig. 6 show that $\Delta G^0 < 0$ since $\ln(K_h) = -\Delta G^0/RT$. The results in Fig. 6 also indicate that in the examined temperature range (295 K–317 K), the ΔG^0 values in general are lower on Au attaining values from −29 kJ/mol to −79 kJ/mol as compared to the situation on HA, where ΔG^0 varies from −13 kJ/mol to −20 kJ/mol. The ΔG^0 values found on Au closely resemble the affinity values which typically are reported in the literature for protein adsorption on 2-D interfaces (−34 kJ/mol to 68 kJ) [20–23], while the values reported on HA are less negative. The smaller ΔG^0 values on HA suggest that OPN binds more weakly to HA in contrast to previous findings [11,12,16,29–32]. From Fig. 6 it is also seen that the ΔG^0 value becomes more negative on both surfaces as the temperature is increased, indicating that the OPN adsorption is endothermic and driven by entropy changes. From Fig. 6 it is also possible to qualitatively determine on which surface the change in entropy is largest. Since the decrease in Gibbs free energy is more dramatic on Au than on HA over the same temperature interval, the data in Fig. 6 tentatively suggest that the entropy change during the adsorption process might be larger on Au as compared to HA, indicating that the individual OPN molecules are most likely adsorbed in a state of higher entropy on Au compared to HA. From Fig. 6 it is therefore plausible to assume OPN attaches with a higher degree of orientational and conformational freedom on Au than on the HA surfaces in accordance with the protein surface mass uptake results in Fig. 4. Considering the lower water content and higher OPN surface mass density in the protein films formed on Au, it is plausible to assume that the OPN molecules change conformation from an extended and unfolded configuration in solution to more random compact protein complexes on the Au surface as compared to the situation on the HA surfaces (see Fig. 7), since some of the water molecules gathered around the hydrophobic patches on OPN are released when these patches come closer to one another during a structural transition to a more compact adsorption structure. This could also account for the larger entropy increase observed on Au both due to the disorder in such systems, but also the structurally induced dehydration may play an important role, since unfolded proteins in solution typically release water molecules when assembled into compact 3-D structures followed by an increase in entropy [54,59].

On the other hand, the OPN molecules most likely remain in an activated configuration similar to the one in solution on the HA surfaces with an intact hydration shell possibly caused by a more specific interaction between OPN and HA, mediated by the HA-binding site on OPN (see Fig. 7). This could explain the larger OPN surface mass densities found on Au and is in agreement with the results in [16], where it is stated that OPN typically adsorbs in its native and unfolded state on HA.

To further test this hypothesis, an antibody-antigen assay was carried out with QCM-D showing that 0.57 ± 0.02 antibodies bound per OPN molecule on HA which was significantly larger than the 0.141 ± 0.004 antibodies found per OPN molecule on Au.[1] These results are in accordance with the proposed scenario with the OPN molecules adsorbing in a more unfolded and activated configuration on HA as compared to Au [8,27,45] (see Fig. 7). In fact, a recent study with the same OPN molecule used in the present study showed that HA surfaces coated with OPN lead to higher osteoblastic motility and cell spreading as compared to OPN coated Au surfaces [60] conforming the results presented herein.

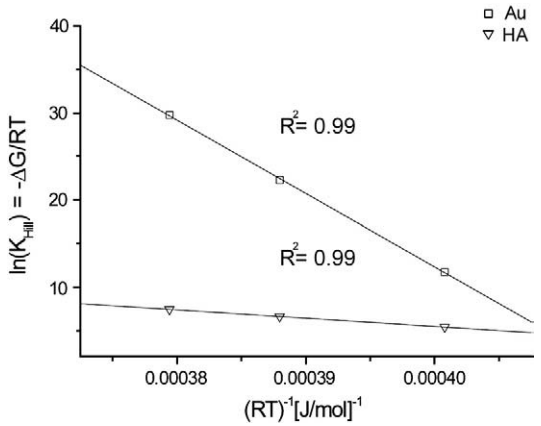

Fig. 6. The changes in $-\Delta G^0/RT$ as a function of (RT^{-1}) for the adsorption of OPN on bare gold (Au) and hydroxyapatite(HA) surfaces.

3.4. The relation between QCM-D dissipation and frequency shift

Additional information on the mechanical and viscoelastic properties of the adsorbed OPN layer can be obtained from the recorded

[1] Test for unspecific antibody binding to the surfaces showed an unspecific binding of less than 8% of the number of antibodies binding per OPN molecule.

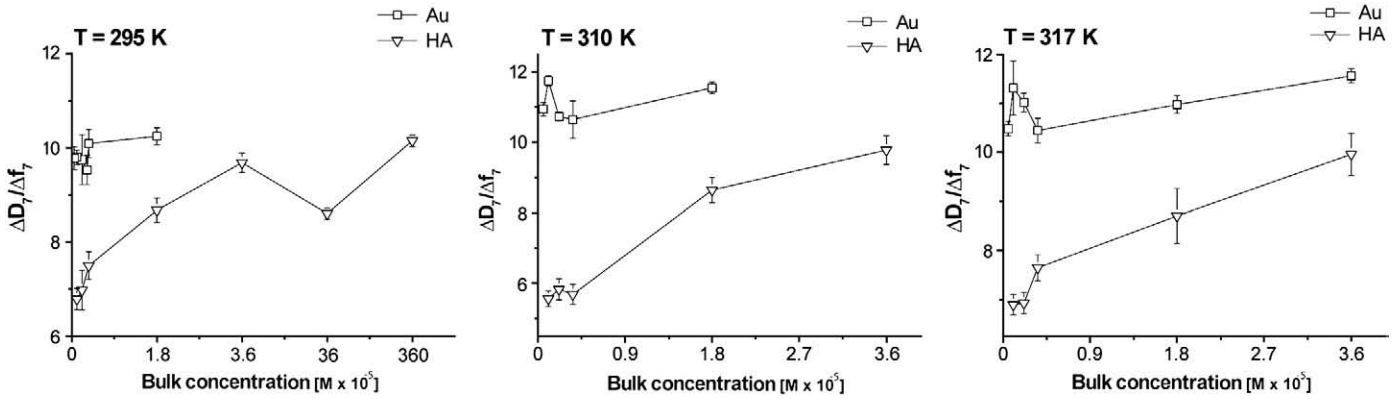

Fig. 8. The dissipation shift per frequency shift ΔD/ΔF obtained for Au and HA at different protein bulk concentrations and temperatures.

ΔD/Δf data [36–39,61–64]. For instance several studies have shown that the ΔD/Δf value increases as the hydration level and flexibility of the protein layer is enhanced [36–39]. In Fig. 8 the ΔD/Δf values are shown at different protein bulk concentrations on Au and HA. The decrease in the ΔD/Δf value as the concentration is lowered is caused by the lower incoming protein flux at the surfaces, which makes it easier for the individual OPN molecules to establish a more rigid coupling to the surfaces. Moreover, the results presented in Fig. 8 show that the ΔD/Δf values in general were largest on Au, which is in accordance with the scenario presented in Fig. 8, where it was concluded that the individual OPN molecules are bound in a more flexible configuration on Au with lower foot-prints value as compared to a more extended and rigid coupling on the HA surfaces. On the other hand the results in Fig. 8 are not in accordance with the assumption that the ΔD/Δf value typically increases concurrently with the hydration level in a protein layer [36,38]. Thus, the QCM-D monitored dissipation values indicate that the flexible OPN configuration on Au is very dissipative and contributes significantly to the ΔD/Δf value, therefore compensating for the lower hydration level in the OPN film formed on Au.

3.5. Conclusion

We have performed an elaborate study of the OPN adsorption on HA and Au. We found that the individual OPN molecules bound in larger quantities on Au than on HA. Moreover, a larger dissipation and lower antibody–antigen recognition was observed on Au as compared to HA. These data altogether suggest that the OPN molecules adsorped to HA in their activated and native configuration, whereas the individual OPN molecules most likely adsorped in more compact protein configurations with lower foot-print values.

Acknowledgement

This study was financially supported by iNANO and the ProSurf research grant from Danish National Advanced Technology Foundation. We would like to thank Kristian Albertsen and Peter Weise, Arla Foods amba for useful discussions and for supplying the OPN, and Esben Skipper Sørensen for supplying the OPN polyclonal antibodies.

References

[1] B.D. Ratner, A.S. Hoffman, F.J. Schoen, J.E. Lemons, Biomaterials Science, 2end ed, San Diego, 2004.
[2] M. Stiehler, M. Lind, T. Mygind, A. Baatrup, A. Dolatshahi-Pirouz, H. Li, M. Foss, F. Besenbacher, M. Kassem, C. Bünger, J. Biomed. Mater. Res. 86A (2007) 448.
[3] R.G.T. Geesink, K.D. Groot, C.P.A.T. Klein, J. Bone. Joint Surg. 70B (1988) 17.
[4] M. Winter, P.P. Griss, K.D. Groot, Biomaterials 2 (1981) 159.
[5] T.W. Bauer, R.G.T. Geesink, R. Zimmerman, J.T. Mcmahon, J. Bone. Joint Surg. 73A (1991) 1439.
[6] M.S. Block, I.M. Finger, M.G. Fontenot, J.N. Kent, Int. J. Oral Maxillofac. Implants 4 (1989) 219.
[7] B. Kasemo, Surf. Sci. 500 (2002) 656.
[8] A. Dolatshahi-Pirouz, T. Jensen, M. Foss, J. Chevallier, F. Besenbacher, Langmuir 25 (2009) 2971.
[9] T. Uemura, Y.K. Liu, Y. Feng, A. Nemeto, T. Yabe, T. Ushida, H. Miyamoto, T. Tateishi, Mater. Sci. Eng. C. 4 (1997) 303.
[10] J. Sodek, B. Ganss, M.D. Mckee, Crit. Rev. Oral Biol. Med. 11 (2000) 279.
[11] F.P. Reinholt, K. Hultenby, Å. Oldberg, D. Heinegård, Proc. Natl Acad. Sci. USA 87 (1990) 4471.
[12] Å. Oldberg, A. Franzen, D. Heinegård, Proc. Natl Acad. Sci. USA 83 (1986) 8819.
[13] K.J. Bayless, G.E. Davis, A.M. Gerald, Protein. Express. Purif. 9 (1997) 309.
[14] A. Franzen, D. Heinegard, Biochem. J. 232 (1985) 715.
[15] E.S. Sørensen, P. Højrup, T.E. Petersen, Protein Sci. 4 (1995) 2040.
[16] L.W. Fisher, D.A. Torchia, B. Fohr, M.F. Young, N. Fedarko, Biochem. Biophys. Res. Commun. 19 (2001) 460.
[17] L. Liu, S. Chen, M.C. Giachelli, B.D. Ratner, S. Jiang, J. Biomed. Mater. Res. 74A (2005) 23.
[18] M.S. Lord, B.G. Cousins, P.J. Doherty, J.M. Whitelock, A. Simmons, R.L. Williams, B.K. Milthorpe, Biomaterials 27 (2006) 4856.
[19] M.T. Bernards, C. Qin, S. Jiang, Colloid. Surface. B 64 (2008) 236.
[20] H. Roos, R. Karlsson, H. Nilshans, A. Persson, J. Mol. Recognit. 11 (1998) 204.
[21] H. Bian, M. Li, Q. Yu, Z. Chen, J. Tian, J.L. Hong, Chem. Pharm. Bull. 54 (2006) 1239.
[22] D.R. Jackson, S. Omanovic, S.G. Roscoe, Langmuir 16 (2000) 5449.
[23] G. Goobes, R. Goobes, W.J. Shaw, J.M. Gibson, J.R. Long, V. Raghunathan, O. Schueler-Furman, J.M. Popham, D. Baker, C.T. Cambell, P.S. Stayton, G.P. Drobny, Magn. Reson. Chem. 45 (2007) S32.
[24] J. Janin, Struct. Funct. Genet. 24 (1996), i.
[25] P. Roach, D. Farrar, C.C. Perry, J. Am. Chem. Soc. 127 (2004) 8168.
[26] A. Dolatshahi-Pirouz, S. Skeldal, M.B. Hovgaard, T. Jensen, M. Foss, J. Chevallier, F. Besenbacher, J. Phys. Chem. C 113 (2009) 4406.
[27] A. Dolatshahi-Pirouz, K. Rechendorff, M.B. Hovgaard, M. Foss, J. Chevallier, F. Besenbacher, Colloid. Surface. B. 66 (2008) 53.
[28] A. Dolatshahi-Pirouz, C.P. Pennisi, S. Skeldal, M. Foss, J. Chevallier, V. Zachar, P. Andreasen, K. Yoshida, F. Besenbacher, Nanotechnology 20 (2009) 095101.
[29] A.M. Pietak, M. Sayer, Biomaterials 27 (2006) 3.
[30] A. Yoshinori, S.R. Rittling, H. Yoshitake, K. Tsuji, K. Shinomiya, A. Nifuji, D.T. Denhardt, M. Noda, Endocrinology 142 (2009) 1325.
[31] L.R. Amir, T. Schoenmaker, V. Everts, A.L.J.J. Bronckers, Cell Tissue Res. 330 (2007) 35.
[32] C. Makiishi-Shimobayashi, T. Tsujimura, A. Sugihara, T. Iwasaki, N. Yamada, N. Terada, M. Sakagami, Hearing. Res. 153 (2001) 100.
[33] E. S. Sørensen, Process for isolation of osteopontin from milk, US patent 7, 259, 243 (21 August 2007)
[34] G. Sauerbrey, Z. Phys. 155 (1959) 206.
[35] M.V. Voinova, M. Rodahl, M. Jonson, B. Kasemo, Phys. Scr. 59 (1999) 391.
[36] F. Höök, B. Kasemo, T. Nylander, C. Fant, K. Sott, H. Elwing, Anal. Chem. 73 (2001) 5796.
[37] F. Höök, J. Vörös, M. Rohdahl, R. Kurrat, P. Böni, J.J. Ramsden, M. Textor, N.D. Spencer, P. Tengvall, J. Gold, B. Kasemo, Colloid. Surface. B. 24 (2002) 155.
[38] J. Vörös, Biophys. J. 87 (2004) 553.
[39] E. Reimhult, C. Larsson, B. Kasemo, F. Höök, Anal. Chem. 76 (2004) 7211.
[40] A. Dolatshahi-Pirouz, M.B. Hovgaard, K. Rechendorff, J. Chevallier, M. Foss, F. Besenbacher, Phys. Rev. B 77 (2008) 115427.
[41] K. Rechendorff, M.B. Hovgaard, J. Chevallier, M. Foss, F. Besenbacher, Langmuir 22 (2006) 10885.
[42] M.S. Lord, B.G. Cousins, P.J. Doherty, J.M. Whitelock, A. Simmons, R.L. Williams, B.K. Milthorpe, Biomaterials 27 (2006) 4856.
[43] A. Posner, A. Perloff, A. Diori, Acta Crystallogr. 11 (1958) 308.
[44] F. Caruso, D. Neil Furlong, P. Kingshott, J. Colloid. Interf. Sci. 186 (1997) 129.
[45] M. Malmsten, Biopolymers at interfaces, 2end ed, Marcel Dekker Inc, New York, 2003.
[46] http://www.lasmea.univ-bpclermont.fr/Personnel/Bernard.Gruzza/IMFP.html.
[47] H. Fisher, I. Polikarpov, A.F. Craivich, Protein Sci. 13 (2004) 2825.

[48] N.P. Cosman, G.S. Sharon, Langmuir 20 (2004) 1711.
[49] H.M. Kowalczynska, M. Nowak-Wyrzykowska, R. Kolos, J. Dobkowski, J. Kaminski, J. Biomed. Mater. Res. 72A (2004) 228.
[50] B.G. Keselowsky, D.M. Collard, A. Garcia, J. Biomed. Mater. Res. 66A (2003) 247.
[51] I.-N. Chang, J.-N. Lin, J.D. Andrade, J.N. Herron, J. Colloid. Interf. Sci. 174 (1995) 10.
[52] S. Kurosawa, N. Kamo, H. Aizawa, M. Muratsugu, Biosens. Bioelectron. 22 (2007) 2598.
[53] Q. Luo, J.D. Andrade, J. Colloid Interf. Sci. 200 (1998) 104.
[54] J. Israelachvili, Intermolecular and Surface Forces, 2end ed.Elsevier, San Diego, 2006.
[55] V.A. Basiuk, T.Y. Gromovoy, Colloid. Surf. B. 118 (1996) 127.
[56] R. Janzen, K.K. Unger, J. Chromatogr. 522 (1990) 77.
[57] D.S. Gill, D.J. Roush, R.C. Willson, J. Colloid Interf. Sci. 167 (1994) 1.
[58] H.P. Jennissen, Biochemstry 15 (1976) 5683.
[59] J.M. Berg, J.L. Tymoczko, L. Stryer, Biochemistry, 5end ed.W. H. Freeman and Company, New York, 2002.
[60] T.H.L. Jensen, A. Dolatshahi-Pirouz, M. Foss, J. Baas, M. Kassem, C. Bünger, K. Søballe, F. Besenbacher, Coll. Surf. B 75 (2009) 186.
[61] F. Höök, M. Rodahl, B. Kasemo, P. Brzezinski, Proc. Natl Acad. Sci. USA 95 (1998) 12271.
[62] M. Rodahl, F. Höök, C. Fredriksson, C.A. Keller, A. Krozer, P. Brzezinski, M. Voinova, B. Kasemo, Faraday Discuss. 107 (1997) 229.
[63] M.S. Lord, M.H. Stenzel, A. Simmons, B.K. Milthorpe, Biomaterials 27 (2006) 1341.
[64] F. Höök, M. Rodahl, P. Brzezinski, B. Kasemo, Langmuir 14 (1998) 729.